

## **Change Detection in Ottawa City Synthetic Aperture Radar Remote Sensing Images based on DWT Fuzzy C Means Clustering**

**J. Thrisul kumar<sup>1</sup>, G.Venu Ratna Kumari<sup>2</sup>, M. Satish kumar<sup>2</sup>, K. Pradeep Vinaik<sup>3</sup>, P. Raju<sup>4</sup>**

<sup>1</sup>Associate Professor, Vignan's Nirula institute of tech and science for women, Guntur, A.P.

<sup>2</sup>Assistant Professor, Dept of Civil Engg, Siddharta Institute of Technology, Vijayawada, A.P.

<sup>2</sup> Professor, Dept of Civil Engg, Kallam Haranatha Reddy Inst of Tech, Guntur, A.P.

<sup>3,4</sup>Assistant Professor, EECE Department, GITAM (Deemed to be university), Visakhapatnam, A.P.

**Corresponding author: kumarthrisul9@gmail.com**

**Abstract:** The radiometric, spectral, spatial and temporal resolutions of remote sensing data have a major effect on the success rate of the applications that deploy remote sensing applications. In the traditional works, the issues related to remote sensing images are usually signified for particular kinds of sensors (that is, active or passive). While deploying passive sensors in remote sensing(e.g., optical images), differentiated image is generally calculated and a suitable measure of change is provided. On the other hand, in rainy or cloudy regions, the exploitation of optical images tends to be limited. From this viewpoint, Synthetic Aperture Radar (SAR) imaging can be regarded as the most excellent substitute for remote sensing applications. In this regard, two multitemporal SAR images have been taken for this fusion process. Usually, the major need of image fusion is to extract the information from multiple images and convert them into one image with all information in individual images. To perform this image fusion multiple wavelet coefficients have been applied in Discrete Wavelet Transform (DWT) such as Daubchies wavelet coefficients (daubchies2) have been used. After performing this fusion, fused image is segmented as changed regions and unchanged regions based on Fuzzy C Means clustering (FCM). the segmented image is compared with the ground truth image the outcome is measured in terms measuring parameters such as accuracy, precision, sensitivity and FDR.

**Key words:** SAR, DWT, Daubechies, accuracy, precision, sensitivity and FDR.

### **1.Introduction**

#### **i) Remote sensing:**

Nowadays, individuals are very much interested in monitoring and observing their neighbour surroundings. "The collection of techniques involved in monitoring objects on the Earth's surface without any physical contact is called remote sensing" [1-4]. The remote sensing methods were developed speedily and it has attained huge attention for observing the earth

surface. The application on remote sensing [5-7] is rapidly growing in recent days owing to the accessibility of a vast range of techniques to achieve the information regarding the earth's surface. In remote sensing,[8][9] the data regarding the earth's surface is gathered through the backscattered or reflected signals.

SAR systems are broadly deployed in remote sensing appliances. It is also deployed in awareness applications at the early stage; however, its use is later extended to other appliances such as archaeology, oceanography, geophysics, etc. The SAR is an airborne framework that travels all along the flight path and generates high image resolution. As mentioned earlier, SAR provides excellent resolution over other radars, owing to the antenna movement with respect to the objects. Particularly, SAR includes the ability to generate the images at all conditions of weather. The first SAR image was captured in 1953 by means of c-46 airborne that could be exploited for observing the west Florida zone. The NASA center has constructed the 1<sup>st</sup> SAR aircraft satellite in 1978. Later, Russia, Europe, and Canada have modelled their specific customary SAR satellite frameworks in 1987, 1991 and 1995 respectively.

## **ii) Synthetic Aperture Radar**

SAR is an airborne radar [10-12], which produce high imagery resolution by creating a flight path that resembles a huge antenna aperture by electronic means. Information from every cycle captivates the transmitting and receiving pulses individually and it stores them electrically. From the successive pulses, the signal processing unit exploits the phase and magnitude of the obtained signals [13] [14]. Following a certain interval, this stored data is merged that forms a high-resolution image of the landscape, which is being flown by means of the Doppler Effect.

The SAR system is also a coherent radar system that is exploited to produce images with high resolutions [15] [16]. The image is generated due to the uninterrupted waveforms, which are transmitted and received via an antenna that moves through the flight path. The phase and magnitude are used for processing the signal. In addition, numerous pulses are transmitted as the spacecraft with the radar [17] [18] moves along a particular path. The image size is based on the transmitted pulse width and distance among the target and transmitted pulse.

SARs usually functions at varying wavelengths that range from 1cm to numerous meters in the microwave region of EM spectrum. This system is a dynamic system since it

releases the EM radiation and evaluates the electric field generated by the backscattering of the ground [19] [20]. The attained measurements are further converted to a high-resolution image accessible throughout both night and day.

The actuality that SARs [21-22] can function at any weather conditions and at any time of the day is due to the fact that earth is almost translucent in microwave areas. The pulses that are transmitted with wavelengths above 1cm could infuse through the smallest available space. Therefore, the process of SAR [23] is feasible even in the existence of rain, cloud or fogs that is a restraining feature in Optical sensing. Thus, SAR is an effectual functioning system that could envelop all the earth surfaces irrespective of operating time [24 -26].

## 2. Image fusion

### 1. ImageFusion:

Imagefusionisthestrategyofmergingtherequiredinformationoftwoormoresourceima  
 gesintoalast intertwined image. Resultant image would be much effective and point by  
 point when compared to any of  
 theinputimages.Bythestrategyimagefusion,theincredibleinformationfromeachofthegiveni  
 mageismelded. Basically, four types of image fusion technique have been opted by  
 many researchers those are given asfollows

#### a) Multi-view ImageFusion:

Thisframeofimagefusionincorporatecombinationoftwoormoresourceimagesataretakesa  
 tthesametime which have that same methodology but distinctive source images are to be  
 taken from different places or completely different foundation conditions.

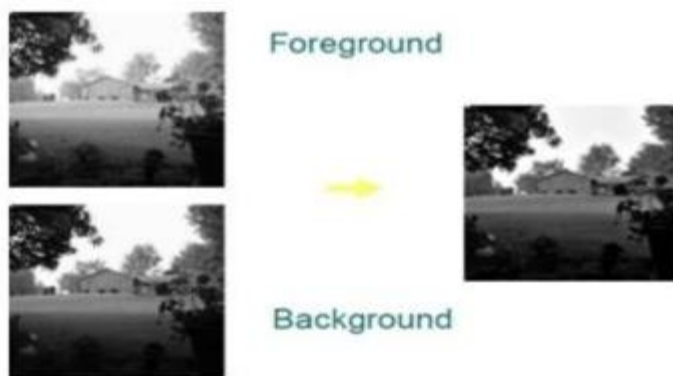


**Fig.1. Representation of Multi-view Image Fusion**

**b) MultimodalFusion:**

This type of fusion uses two or more images that include different modalities and the object. Mostly this kind of fusion uses in Bio-Medical applications such as MRI, CTscan.

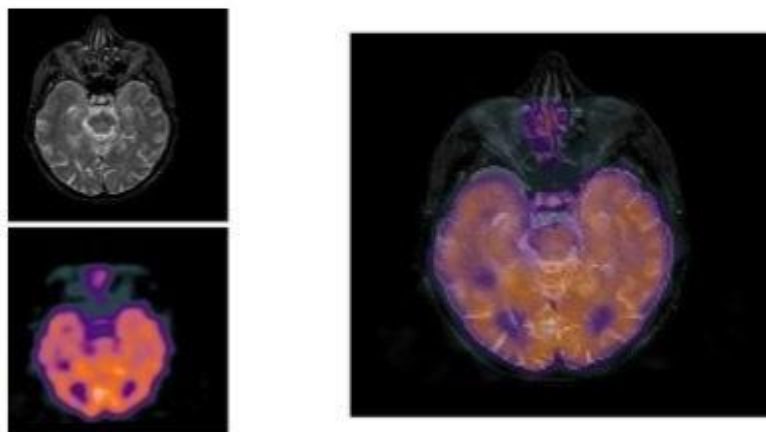


**Fig.2. Representation of Multimodal Fusion**

**c) Multi-temporalFusion:**

This type of fusion uses two or more images that capture the same object at different timings. Mostly this kind of fusion uses in remote sensing applications such as SAR image processing.



**Fig.3. Representation of Multi-temporal Fusion**

Multi-focus Fusion: this type of fusion will be performed by two or more source images where each source image is divided into areas such that every pixel is in focus at least in a

## 2. Discrete Wavelet Transform

Typically, DWT [7-12] is any wavelet transform in numerical or functional evaluation where the wavelets are discretely evaluated. Among all the wavelet transforms, DWT is significant as it takes both frequencies as well as location data. Here in this research work, the images are processed by transmitting them using an AFB followed by a decimation function in DWT. The AFB contains an HPF and an LPF, which are normally utilized for image compression. The image is divided as 2 bands while it is transmitted through AFB. Moreover, the HPF is coupled with a differencing function, which extracts detailed information regarding the image data. On contrast to HPF, LPF is associated with an averaging function that attains the whole data about the image. In the meantime, the filtering function output is continuously decimated by 2, Eq. (1) expresses the mother wavelet, in which  $v$  signifies coefficient of shifting and  $u$  specifies coefficient of scaling. The whole other fundamental functions are taken as the mother wavelet's differentiation.

$$\Gamma_{u,v}(m) = \frac{1}{\sqrt{u}} \Gamma\left(\frac{m-v}{u}\right) \quad (1)$$

Generally,  $(\psi(m, n))$  is 2D scaling function and  $[\Gamma^A(m, n), \Gamma^B(m, n), \text{ and } \Gamma^C(m, n)]$  are three 2D wavelets are required in 2D DWT process. Moreover, all the components are products of 1D scaling function  $\psi$  and its corresponding wavelet  $\Gamma$ . Despite the products that produce 1D result like  $\Gamma(m)$ ,  $\psi(m)$  the resultant four products produce the independent scaling function as defined in Eq. (2), and Eq. (3). Eq. (4) and Eq. (5) states the independent, directional sensitive wavelets respectively.

$$\psi(m, n) = \psi(m) \psi(n) \quad (2)$$

$$\Gamma^B(m, n) = \psi(m) \Gamma(n) \quad (3)$$

$$\Gamma^A(m, n) = \Gamma(m) \psi(n) \quad (4)$$

$$\Gamma^C(m, n) = \Gamma(m) \Gamma(n) \quad (5)$$

Typically, the abovementioned wavelets determine functional differences, gray level deviations, or image intensity in different directions. Moreover,  $\Gamma^B$  determines the variations with horizontal edges or columns,  $\Gamma^A$  is related to differences with vertical edges or rows, and  $\Gamma^C$  signifies the variations with diagonals. In addition to this, translated as well as scaled basis functions are stated in Eq. (6) and Eq. (7) respectively, while index 'a' identifies Directional

wavelets and 'b' specifies the scaling function. Here, Eq. (8) and Eq. (9) specifies the determination of DWT of image  $g_i(m, n)$  with size  $X \times X$ .

$$\psi_{b,x,x}(m, n) = 2^{\frac{b}{2}} \psi(2^b m - x, 2^b n - x) \quad (6)$$

$$\Gamma_{b,x,x}^a(m, n) = 2^{\frac{b}{2}} \Gamma^a(2^b m - x, 2^b n - x), a = \{B, A, C\} \quad (7)$$

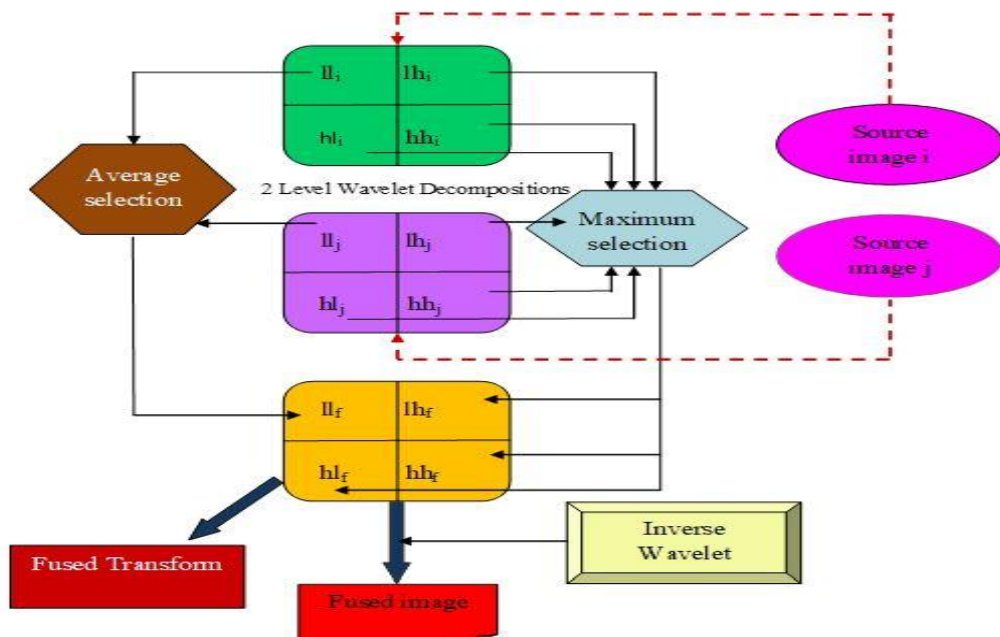
$$\Gamma_{\psi}(b_0, x, x) = \frac{1}{\sqrt{XX}} \sum_{m=0}^{X-1} \sum_{n=0}^{X-1} g_i(m, n) \psi_{b_0,x,x}(m, n) \quad (8)$$

$$\Gamma_{\psi}^a(b, x, x) = \frac{1}{\sqrt{XX}} \sum_{m=0}^{X-1} \sum_{n=0}^{X-1} g_i(m, n) \Gamma_{b,x,x}^a(m, n) \quad (9)$$

Eq. (10) shows the wavelet  $Z_D(\hat{g}_i)$  combined to the input image in DWT, and  $M_c$  refers to the optimized filter coefficient. Eq. (10) and Eq. (11) are utilized to analyse the inverse DWT and its execution can be referred using Eq. (11).

$$Z_D(\hat{g}_i) = \sum_j M_c \psi(2\hat{g}_i - D) \quad (10)$$

$$g_i(m, n) = \frac{1}{\sqrt{XX}} \sum_x \sum_x \Gamma_{\psi}(b_0, x, x) \psi_{b_0,x,x}(m, n) + \frac{1}{\sqrt{XX}} \sum_{a=B,A,C} \sum_{b=b_0}^{\infty} \sum_x \sum_x \Gamma_{b,x,x}^a(m, n) \quad (11)$$



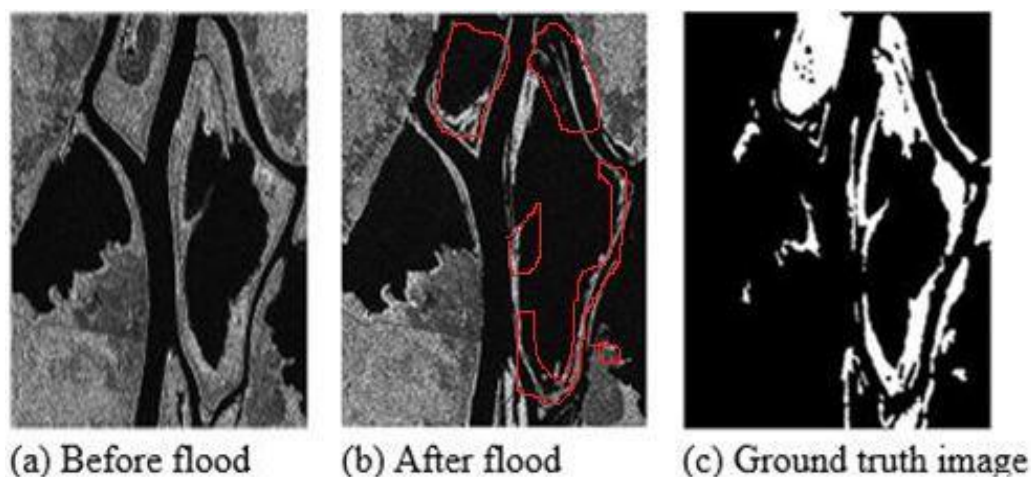
**Fig. 4. The overall architecture of the DWT-based image fusion model**

Fig. 4 specifies the overall architecture of the DWT-based image fusion model having two source images along with the average selection and maximum selection processes. The overall procedures included in DWT-based image fusion model are explained in the following steps.

- Attain the 2 source images  $i$  and  $j$  for fusion procedure.
- Perform wavelet decomposition to the input images  $i$  and  $j$  with multiple wavelet coefficients such as Daubchies wavelet coefficients, Symlets and Haar wavelets.consequently, the high frequency(lh),(hl) and (hh) as well as low-frequency components(ll)are attained.
- Compute the average selection procedure, in which the low-frequency images are given to the average selection.
- Compute minimum or maximum selection model, in which a selection procedure is performed to each corresponding pixel of the input images  $i$  and  $j$ . Furthermore, the pixel having low of high intensity is selected respectively.
- Execute inverse DWT on fusedll<sub>f</sub>,lh<sub>f</sub>, hl<sub>f</sub>and hh<sub>f</sub> coefficients for obtaining the fused intensity image.
- Eventually, the novel intensity coordinate of the image is obtained.

### 3. Results and Discussions

Two multi temporal images have been taken for this fusion process .These two images are applied as input to DWT process and multiple wavelts have been used for image fusion. In this paper to endorse the performance of the proposed methodology over the conventional method (image fusion with Daubechies wavelets) satellite images with SAR, sensors have been taken into account. Ottawa data set is taken as data set to validate the proposed methodology. As illustrated in fig.5 two images are processed for fusion, fig 5. (a) represents the image before flood occurs and fig 5 (b) represents the image after the flood is occurred and red colour shows the affected areas. Here the need of fusion is for further processing of these images such as clustering and change detection applications.



**Fig .5. Input data images (a) Before flood (b) After flood (c) Ground truth image**

The fusion process using DWT is implemented by using Daubechies wavelet coefficients from and the resulting fused images is shown in fig 6. (a). After fusion image is segmented by using fuzzy c- means clustering. The Segmented image is compared with the ground truth image and the performance of DWT\_FCM is measured in terms of accuracy, sensitivity, precision and False Detection Rate (FDR).

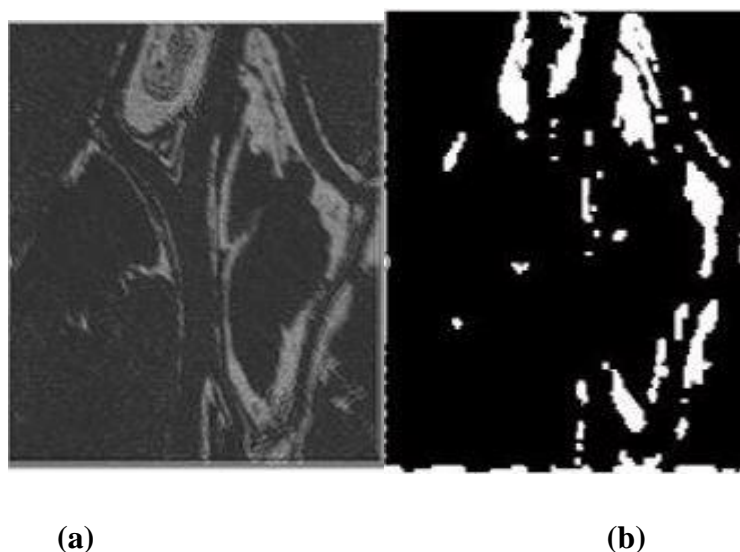


**Fig .6. a) Fused image b) Segmented image**

Measure	FCM_DWT
accuracy	0.9856
sensitivity	0.8919
specificity	0.9857
precision	0.0609



FPR	0.0143
FNR	0.1081
FDR	0.9391
NPV	0.9857
MCC	0.2309
F1-score	0.1140

**Table 1: Performance analysis of the DWT\_FCM**

#### 4. Conclusion

In this paper change detection in SAR images has been implemented through image fusion and FCM clustering. DWT has been employed for fusion of two SAR images to extract the spatial information and spectral information from the two remote sensing images. Clustering has been performed based on soft fuzzy FCM clustering technique. The segmented image is compared with the ground truth image to compare the performance of DWT\_FCM. The implemented method is given good accuracy and small FDR.

#### References:

- [1] Chang-an LIU, Zhong-xin CHEN, Yun SHAO, Jin-song CHEN, Hai-zhu PAN, “Research advances of SAR remote sensing for agriculture applications: A review”, Journal of Integrative Agriculture, vol. 18, no. 3, pp. 506-525, March 2019.
- [2] Xuqing Li, Long Li, Xiangnan Liu, “Collaborative inversion heavy metal stress in rice by using two-dimensional spectral feature space based on HJ-1 A HSI and radarsat-2 SAR remote sensing data”, International Journal of Applied Earth Observation and Geo information, vol. 78, pp. 39-52, June 2019.
- [3] Deodato Tapete, Francesca Cigna, “Trends and perspectives of space-borne SAR remote sensing for archaeological landscape and cultural heritage applications”, Journal of Archaeological Science: Reports, vol. 14, pp. 716-726, August 2017.
- [4] Yanling Du, Wei Song, Qi He, Dongmei Huang, Chen Su, “Deep learning with multi-scale feature fusion in remote sensing for automatic oceanic eddy detection”, Information Fusion, vol. 49, pp. 89-99, September 2019.

- [5] Yue Wu, Wenping Ma, Qiguang Miao, Shanfeng Wang, “Multimodal continuous ant colony optimization for multisensor remote sensing image registration with local search”, *Swarm and Evolutionary Computation*, vol. 47, pp. 89-95, June 2019.
- [6] Jianxiu Qiu, Wade T. Crow, Wolfgang Wagner, Tianjie Zhao, “Effect of vegetation index choice on soil moisture retrievals via the synergistic use of synthetic aperture radar and optical remote sensing”, *International Journal of Applied Earth Observation and Geoinformation*, vol. 80, pp. 47-57, August 2019.
- [7] Thrisul Kumar Jakka, Y. Mallikarjuna Reddy , B. Prabhakara Rao “GWDWT-FCM: Change Detection in SAR Images Using Adaptive Discrete Wavelet Transform with Fuzzy C-Mean Clustering” *Journal of the Indian Society of Remote Sensing* (March 2019) 47(3):379–390.
- [8] J. Thrisul Kumar, Y. Mallikarjuna Reddy, B. Prabhakara Rao “Image Fusion of Remote Sensing Images using ADWT with ABC Optimization Algorithm”, *International Journal of Innovative Technology and Exploring Engineering (IJITEE)* ISSN: 2278-3075, Volume-8 Issue-11, September 2019
- [9] J. Thrisul Kumar, Y. Mallikarjuna Reddy, B. Prabhakara Rao “Change Detection in Sarimages Based on Artificial Bee Colony Optimization With fuzzy C - Means Clustering” *International Journal*
- [10] J. Thrisul Kumar, Y. Mallikarjuna Reddy, B. Prabhakara Rao “WHDA-FCM: Wolf Hunting-Based Dragonfly With Fuzzy C-Mean Clustering For Change Detection In SAR Images” *Section B: Computer and Communications Networks and Systems*
- [11] J. Thrisul Kumar, Y. Mallikarjuna Reddy, B. Prabhakara Rao “Change Detection in Sar images Based on Artificial Bee Colony Optimization with Fuzzy C - Means Clustering”, *International Journal of Recent Technology and Engineering (IJRTE)*, ISSN: 2277-3878, Vol -7 Issue-4, Nov 2018, pp- (156- 160)
- [12] .J.Thrisul Kumar, N.Durgarao, E.T.Praveen, M.Kranthi Kumar “ Modified Image Fusion TechniqueFor Dual-Tree Complex Wavelet Transform” *International Journal Of Advanced Science And Technology* , Vol. 29, No. 5s, (2020), pp. 895-901

- [13] Yuanzhi Zhang, Hongsheng Zhang, Hui Lin, "Improving the impervious surface estimation with combined use of optical and SAR remote sensing images", *Remote Sensing of Environment*, vol. 141, pp. 155-167, 5 February 2014.
- [14] Amit Kumar, B. S. P. C. Kishore, P. Saikia, J. Deka, M. L. Khan, "Tree diversity assessment and above ground forests biomass estimation using SAR remote sensing: A case study of higher altitude vegetation of North-East Himalayas, India", *Physics and Chemistry of the Earth, Parts A/B/C*, vol. 111, pp. 53-64, June 2019.
- [15] Shuang Wang, Dou Quan, Xuefeng Liang, Mengdan Ning, Licheng Jiao, "A deep learning framework for remote sensing image registration", *ISPRS Journal of Photogrammetry and Remote Sensing*, vol. 145, Part A, pp. 148-164, November 2018.
- [16] C. McGuinness and E. Balster, "Enabling Reliable Change Detection for Independently Compressed SAR Images," *IEEE Transactions on Geoscience and Remote Sensing*, vol. 55, no. 8, pp. 4785-4794, Aug. 2017.
- [17] T. L. M. Barreto et al., "Classification of Detected Changes From Multitemporal High-Res Xband SAR Images: Intensity and Texture Descriptors From SuperPixels," *IEEE Journal of Selected Topics in Applied Earth Observations and Remote Sensing*, vol. 9, no. 12, pp. 5436-5448, Dec. 2016.
- [18] A. Kim, K. Lee, B. Kim, W. Lee and J. Baek, "Development of change detection algorithm using high resolution SAR complex image," 2015 IEEE 5th Asia-Pacific Conference on Synthetic Aperture Radar (APSAR), Singapore, pp. 822-826, 2015.
- [19] A. Thayalan, F. S. Abas and V. C. Koo, "Automatic change detection of Belum-Temengor forested area using multitemporal SAR images," *IEEE International Conference on Signal and Image Processing Applications*, Kuala Lumpur, pp. 318-321, 2009.
- [20] Yaoguo Zheng, Licheng Jiao, Hongying Liu, Xiangrong Zhang, Biao Hou and Shuang Wang, "Unsupervised saliency-guided SAR image change detection," *Pattern recognition*, vol. 61, pp. 309-326, January 2017.
- [21] K. W. Lee, H. Kim, B. Kim and W. Lee, "Design of SAR image feature detector for small-scaled coherent change detection," *IEEE International Geoscience and Remote Sensing Symposium (IGARSS)*, Beijing, pp. 2344-2347, 2016.
- [22] M. Gong, L. Su, M. Jia and W. Chen, "Fuzzy Clustering With a Modified MRF Energy Function for Change Detection in Synthetic Aperture Radar Images," *IEEE Transactions on Fuzzy Systems*, vol. 22, no. 1, pp. 98-109, Feb. 2014.

- [23] Shang Ronghuaa, Yuan Yijinga, Jiao Lichenga, Meng Yanga and Amir Masoud Ghalamzan, "A self-paced learning algorithm for change detection in synthetic aperture radar images," *Signal processing*, vol. 142, pp. 375-387, January 2018.
- [24] M. Gong, J. Zhao, J. Liu, Q. Miao and L. Jiao, "Change Detection in Synthetic Aperture Radar Images Based on Deep Neural Networks," *IEEE Transactions on Neural Networks and Learning Systems*, vol. 27, no. 1, pp. 125-138, Jan. 2016.
- [25] Turgay Celik, "A Bayesian approach to unsupervised multiscale change detection in synthetic aperture radar images," *signal processing*, vol. 50, no. 5, pp. 1471-1485, May 2010.
- [26] F. Gao, J. Dong, B. Li and Q. Xu, "Automatic Change Detection in Synthetic Aperture Radar Images Based on PCANet," in *IEEE Geoscience and Remote Sensing Letters*, vol. 13, no. 12, pp. 1792-1796, Dec. 2016.
- [27] S. Cui, G. Schwarz and M. Datcu, "A Benchmark Evaluation of Similarity Measures for Multitemporal SAR Image Change Detection," in *IEEE Journal of Selected Topics in Applied Earth Observations and Remote Sensing*, vol. 9, no. 3, pp. 1101-1118, March 2016.
- [28] V. Bhavana and H. K. Krishnappa, "Fusion of MRI and PET images using DWT and adaptive histogram equalization," *2016 International Conference on Communication and Signal Processing (ICCSP)*, Melmaruvathur, pp. 0795-0798, 2016.
- [29] X. Zhang, H. Li and L. Jiao, "A change detection algorithm based on object feature for SAR image," *2009 2nd Asian-Pacific Conference on Synthetic Aperture Radar*, Xian, Shanxi, pp. 693-696, 2009.